5th Joint International Symposium on Deformation Monitoring (JISDM), 20-22 June 2022, Valencia, Spain
DOI: http://doi.org/10.4995/JISDM2022.2022.13844

Including virtual target points from laser scanning into the point-wise rigorous deformation analysis at geo-monitoring applications

Lukas Raffl, Christoph Holst

Chair of Engineering Geodesy, TUM School of Engineering and Design, Technical University of Munich, 80333 München, Germany, (lukas.raffl@tum.de; christoph.holst@tum.de)

Key words: *point clouds; deformation vectors; virtual targets; congruence model; scanning total station*

ABSTRACT

We present a method to include virtual target points from laser scanning into the point-based rigorous deformation analysis to derive precise 3D deformation vectors. This method overcomes the challenge of missing point identities in laser scans and is developed especially for geo-monitoring applications that demand an early identification of deformations at previously unknown positions. Our approach is based on virtual targets represented by local scan patches. Each patch is matched between overlapping stations and across different measurement epochs using the Iterative Closest Point Algorithm (ICP). Thus, similar to feature points, a number of homologous points is created and polar pseudo-observations are derived. This allows to integrate the observations into a free network adjustment and into a rigorous deformation analysis. We apply this method to the geo-monitoring of rock surfaces on Mt. Hochvogel where we use a scanning total station combining point-wise measurements to signalized targets and pseudo-observations derived from area-wise laser scans. In our application, numerous virtual target points could be created throughout the deformation object. The results show that the new method improves the accuracy and reliability of the subsequent rigorous deformation analysis and it, thus, allows for an early identification of deformations at geo-monitoring applications. Still there is some improvement in the selection of suitable patches needed, as the matching accuracy of the ICP strongly depends on the point distribution within the patches.

I. INTRODUCTION

Geo-monitoring is one aspect of risk prevention in the alpine regions. Nowadays, terrestrial laser scanners are frequently used not only to monitor deformations of infrastructural buildings (Mukupa *et al.*, 2016), but also deformations in the context of those geo-applications, such as landslides (Kromer *et al.*, 2017; Pfeiffer *et al.*, 2018), rockfalls (Kenner *et al.*, 2022; Abellán *et al.*, 2011), solifluctional processes (Holst *et al.*, 2021) or other mass movements (*e.g.*, Anders *et al.*, 2021). The broad use of laser scanner point clouds for those applications can be reasoned by the fact that point clouds provide a nearly continuous digitalization of the reality that allows for detecting geometric changes with high spatial resolution.

However, for a reliable quantification of potentially existing deformations, a rigorous deformation analysis is needed that also relies on a straightforward and comprehensive error propagation. The implementation of such a rigorous strategy is currently focused in many publications using different methods (*e.g.*, Winiwarter *et al.*, 2021; Wunderlich *et al.*, 2020). Within this topic, our study will show first results of a new method that combines point-wise measurements of a total station with laser scans in a rigorous deformation analysis. Precisely, we will:

- Extend point-wise measurements by small-scale laser scans;
- Extract virtual target points from those point clouds and integrate them into the network adjustment and subsequent deformation analysis;
- Apply the method to a rockfall at Mt. Hochvogel and;
- Identify the limits of our method and propose possible solutions for those limits.

In this context, Section II recapitulates the state of the art related to our strategy, Section III introduces our strategy that is applied to a landslide at Mt. Hochvogel in Section IV. Section V discusses the results and Section VI provides a conclusion and outlook.

II. BASICS OF RELATED STRATEGIES FOR DEFORMATION ANALYSIS

The aim of geodetic monitoring is to determine geometrical deformations in shape or position of an object between two measurement epochs (Heunecke *et al.*, 2013). Besides the quantification of geometric changes also the identification of its statistical significance based on the measurement uncertainties is a major part of the deformation analysis in engineering geodesy (Kuhlmann *et al.*, 2014). Depending on the desired aim of the deformation analysis, different deformation models might be chosen that differ in the fact whether they integrate the acting force and whether they explicitly model the time as variable or not (Welsch and Heunecke, 2001). If neither acting forces are measured nor does exist a long history of epochs, the congruence model is chosen. This also holds for many geo-monitoring applications.

Since Pelzer (1971), the standard process of geodetic deformation analyses within the congruence model is based upon measuring signalized points, estimating their coordinates using a network adjustment and identifying their stability or their movement using a significance test. While this strategy is timelessly suited to provide reliable results for those individual signalized points, it currently fails when trying to integrate laser scans due to two reasons (Holst and Kuhlmann, 2016):

a) Firstly, individual points within laser scans cannot be estimated based upon a network adjustment straightforward due to missing point identities.
b) Secondly, the stochastic model of laser scans is more complex than the one of point-wise measurements as, *e.g.*, of total stations. Thus, a comprehensive assessment of all relevant errors is a broad research topic for itself (Medić *et al.*, 2020; Wujanz *et al.*, 2017).

Consequently, for point-cloud-based monitoring, different strategies evolved (Lindenbergh and Pietrzyk, 2015; Neuner *et al.*, 2016). Herein, point clouds are compared, *e.g.*, based on the M3C2 algorithm (Lague *et al.*, 2013; Winiwarter *et al.*, 2021), best-fitting surfaces from triangulation (Akca, 2007; Ge, 2016) or free-form parametrizations (Harmening and Neuner, 2016), or geometrical primitives (Holst *et al.*, 2012; Scaioni *et al.*, 2014). Alternatively, the point clouds are reduced to individual points that can be found again in each epoch. This makes it possible to integrate them into the standard procedure according to Pelzer (1971). One strategy to create corresponding points is to interpolate the irregular point clouds of all epochs to the same regular grid (Schäfer *et al.*, 2004). However, because of the grid interpolation displacements are only detectable in one dimension and no actual 3D deformation vectors can be derived. Individual points can also be modelled by estimating and intersecting planes (Raffl *et al.*, 2019), but this approach is limited on a specific surface geometry. More suitable for irregular rock faces is the extraction of corresponding feature points, either based on machine learning (Gojcic *et al.*, 2019) or on additional RGB images (Wagner, 2016). Furthermore, features can be extracted from the 2D representation of a digital elevation model (DEM) created from the laser scans for each epoch (Holst *et al.*, 2021).

A special case of point-cloud-based monitoring is subdividing the point cloud into patches using the iterative closest point algorithm (ICP, Besl and McKay, 1992) as is done in the ICProx (Wujanz, 2016). This is very suitable for irregular structures and therefore for the monitoring of landslides and rockfalls (Pfeiffer *et al*. 2018). The patches can even be seen as virtual target points (Frangez *et al.*, 2020; Raffl *et al.*, 2019).

For the present study, we implemented a combination of those approaches that reduces the point cloud to individual patches that are integrated into the point-wise deformation analysis according to Pelzer (1971). This reduction to patches either allows to compare point identities (aspect a) and it as well simplifies the determination of the measurements' stochastic model within the deformation analysis (aspect b).

III. Methodology

We introduce an extended network-based monitoring strategy. On top of traditional network observations like tacheometric or GNSS baseline observations, scan patches are included as non-signalized target points. By raising the number of potential object points, this novel method makes it possible to (i) increase the spatial coverage also in inaccessible areas and to (ii) improve the network geometry. In this section, we describe the workflow for the integration of virtual target points from laser scanning into the rigorous deformation analysis based on ICP matching. This workflow was specially developed for scanning total stations where the resulting point clouds are already georeferenced via the stationing of the instrument, but it is also transferable to laser scanner data.

A. *ICP Matching*

Non-signalized targets are represented by small-scale laser scanning patches. Each patch defines one virtual target point and has a typical diameter of 0.3 to 0.5 m. In the zero epoch, for each patch a master point cloud is captured and the coordinates of the virtual target point $\mathbf{P_0}$ are assigned (*e.g.*, the centroid of the patch) (Figure 1a). The same patches are then scanned in all following measurement epochs.

Under the assumption that the inner geometry of each patch is not changing over time, its rigid-body movement between two epochs can be determined by a classical cloud-to-cloud matching based on the ICP algorithm. Neglecting an eventual registration error, the ICP already gives the rigid-body movement of the patch between the epochs. However, no reliable stochastic model for the deformation vector is available. Therefore, in a first step, we use the result of the ICP matching to create point identities between the two epochs. By applying the resulting transformation $\mathbf{T}$ on the virtual point $\mathbf{P_0}$ of the zero epoch, it is transferred into the current epoch creating the point $\mathbf{P_1}$ and thus a pair of corresponding points (Figure 1a).

With this strategy, point identities can not only be created across different epochs, but also between two stations, creating redundancy within one epoch (Figure 1b). The procedure is the same, however, when scanning from two different instrument stations, it must be ensured that the ICP matching gives reliable results despite different viewing angles.

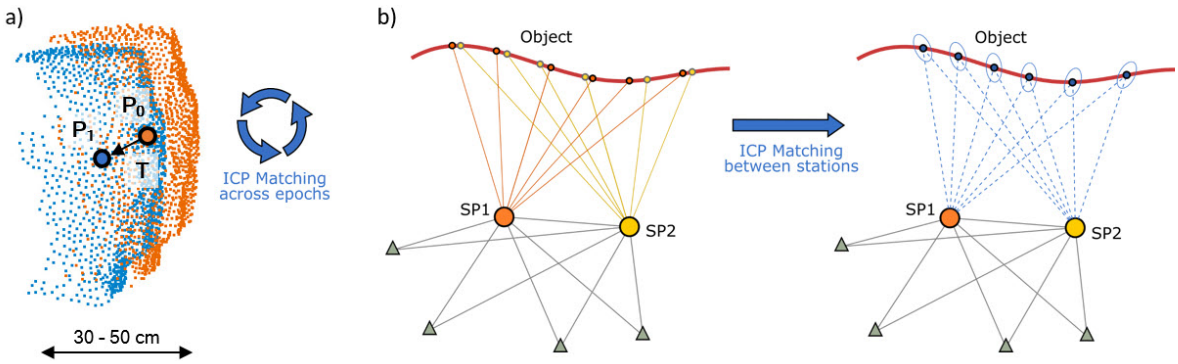

Figure 1. a) ICP matching across two epochs and updating the virtual point; b) ICP matching between two stations and integration into the geodetic network consisting of control points (triangles) and object points (circles).

B. *Network adjustment and deformation analysis*

Creating point identities between different stations and across different epochs enables the integration of the virtual target points into the network adjustment and the network-based deformation analysis. For this purpose, polar single-point observations are derived. Considering the related station coordinates for each virtual point, a pseudo-observation is determined composed of horizontal angle, vertical angle and slope distance, identical to a tacheometric observation. These are now treated as conventional polar observations and combined with other network observations like actual total station measurements to signalized points or GNSS baseline observations. In general, the datum is realised by a set of stable control points observed with GNSS.

All network measurements of one epoch are then evaluated in a hybrid free network adjustment, whereby individual variance components are estimated for each of the different observation types (Heunecke *et al.*, 2013; Niemeier, 2008). If the virtual points are observed from more than one station, their variance level is automatically adapted to the actual observation quality based on the resulting redundancy within the network adjustment. Thus a comprehensive a priori error propagation can be omitted. In the following rigorous deformation analysis, the accuracy information is then used to perform a statistic significance test for all calculated deformation vectors.

In general, the additional non-signalized points help to improve the network geometry and may improve the overall variance level. Consequently, also the sensitivity towards the detection of significant deformations may become higher, and thus eventual displacements of the monitoring object might be revealed earlier.

As mentioned, the here introduced simple approach of converting the updated point coordinates into tacheometric pseudo-observations is especially useful for scanning total stations. In this case, the point clouds are levelled, which is necessary to distinguish correctly between horizontal and vertical angle within the calculation of the pseudo-observations. Furthermore, the registration of the laser scans is already solved through the stationing of the total station.

Consequently, when using a laser scanner, the point clouds need to be levelled as well in order to derive correct pseudo-observations. This can be realized either by precise levelling of the laser scanner or solving the rotation via registration points. If hybrid network measurements are carried out, pseudo-observations to registration points are also needed to connect the virtual laser scanner network to the total station and GNSS network. In all cases a rough registration of the laser scans is sufficient, as within the network adjustment the station coordinates may be corrected and thus implicitly also the registration of the point clouds is improved.

IV. Application at the Geo-Monitoring on Mt. Hochvogel

In this section, we present the application of our combined method at the geo-monitoring of Mt. Hochvogel. After introducing the study area, we explain the data acquisition and evaluation process and finally show the results of the combined deformation analysis and improvements we gained by the inclusion of laser scan data.

A. *Study area*

Mt. Hochvogel is located in the south of Germany directly on the border to Austria. With an altitude of 2,592 m a.s.l., it is the highest summit of the surrounding mountains and therefore exposed to strong erosion. Over the last decades, an enormous cleft has formed right on the summit, splitting the entire mountain top into two parts (Figure 2).

Consequently, on the southern part, an estimated volume of up to 260,000 m^3 threatens to break off and fall on the Austrian side. The main fissure opens up by several millimetres per month and to date already extend over a length of about 35 m in the SW-NE direction and is gaping more than 5 m at its widest points. Besides, there are several smaller fissures showing high opening rates as well and making the modelling of the failure process more complicated (Leinauer *et al.*, 2020).

In order to better understand the present failure process and to implement an early warning system, several measurement systems were set up on the mountain including a geodetic monitoring network (Raffl and Wunderlich, 2020).

Figure 2. The summit of Mt. Hochvogel (2,592 m a.s.l.), located on the German-Austrian border, with its enormous cleft. The southern part (left part in the image) is moving several mm per month and threatens to break off completely.

B. *Geodetic network and observations*

The deformation monitoring carried out on the summit of Mt. Hochvogel is based on conventional geodetic network observations. The network-based monitoring combining tacheometric measurements and GNSS baseline observations allows determining precise 3D vectors within a deformation analysis based on the congruence model.

Problems occur as traditionally all network points have to be marked. Especially the moving part of the summit is only reachable by abseiling, which makes the point installation difficult and dangerous. Nonetheless, a number of object points could have been installed in the hazardous area, mainly signalized by permanently remaining reflective tapes. An overview of the marked network points in the area of the main fissure is given in Figure 3. Most points on the northern side of the cleft can be considered stable whereas all points on the southern part are moving. More control points are located at a larger distance.

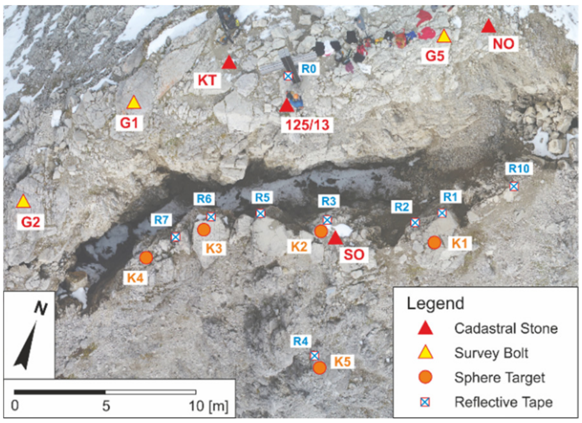

Figure 3. Overview of the marked geodetic network points in the vicinity of the main fissure.

In all measurement epochs, GNSS baseline observations and total station measurements are carried out. With this setup, the network points can be determined with an accuracy of 2-3 mm.

C. *Extension by small-scale laser scans*

In order to increase the spatial resolution on the moving side, the point network is extended by non-signalized object points. For the network measurements, a Leica Nova Multistation MS60 is used, which is an Image Assisted Scanning Total Station (IASTS). Therefore, it can be also used to capture laser scans of the moving southern part of the main fissure. There are two thinkable strategies of capturing a number of patches on the object:

a) Scanning the whole object and clipping suitable patches in the post-processing, or;
b) Already preselecting possible structures in the field and only scanning those selected patches (especially suitable for scanning total stations).

We decided to follow option a) and scanned the entire rock face from two stations: station 1 on G1 and station 2 on NO. The average scan resolution in both scans is about 1 cm on the object, whereby the two point clouds are not overlapping completely. In the scans of the zero epoch a total of 23 patches were manually selected (Figure 4). Hereby, structures like single blocks were chosen where no inner deformation is expected. The patches have a diameter of 0.3 to 0.5 m. However, the measurement configuration is not optimal as the viewing angle from the two stations on the object varies about 90°. This is desirable for the network geometry, but depending on the structures geometry the ICP matching between the stations is more likely to fail because of lower overlapping. Consequently, some of the virtual targets are observed only from one station (blue patches: station 1, yellow patches: station 2) and some from both stations (green patches).

After matching the patches between the two stations and across all epochs, the pseudo-observations are added to the belonging networks. Thus, the number of object points in the hardly accessible area could be raised significantly and the spatial resolution has increased.

D. *Results*

The first complete measurement epoch was carried out in September 2018 and the second followed in July 2019. Besides the marked points, the 23 patches depicted in Figure 4 were observed. The deformation analysis between those two epochs reveals almost no vertical movements but a significant opening of the cleft in horizontal direction. Figure 5 shows the deformation vectors in the horizontal plane. The blue lines represent the measurement network that underlies the deformation analysis. The black arrows visualize the deformations of marked points, whereas the green arrows depict the movements of the non-signalized virtual target points. In the time between the two epochs, the horizontal movement of the object points on the southern part of the summit was about 21 mm.

The accuracy of the horizontal deformation vectors is represented by the red error ellipses and lays between 1-3 mm. Consequently, all shown deformation vectors are significant based on a significance level of 95 %. Regarding the orientation of the error ellipses it can be seen that the in-line-of-sight accuracy of the virtual targets is higher than that of the signalized points. This can be explained by a good ICP matching accuracy in line of sight and the fact that distance measurement noise is reduced due to the large number of points that is used within the matching. However, the angular accuracy of both observation types is quite similar, because of the lower in-plane matching accuracy of the ICP. In overall, the accuracy of the non-signalized points is slightly better than the accuracy of the signalized points. Furthermore, the non-signalized points give the same deformation results in direction and magnitude as the marked points. That can be seen as a first proof for the validity and precision of the approach for geo-monitoring applications.

V. Discussion

The results at Mt. Hochvogel are a first proof of our concept. However, the movement on Mt. Hochvogel mostly occurs in direction of the surface normal. In this case, also the M3C2 algorithm would give good results (Holst *et al.*, 2017). Nonetheless, we showed that the extension by small-scale laser scans works for the monitoring on Mt. Hochvogel. The number of object points in the inaccessible part of the summit could have been raised, which allows getting a more detailed picture of the deformation process. For almost every single rock, a precise 3D deformation vector can be determined.

The strength of the method is that point identities are created, also between two or more stations of the same epoch. In comparison to feature-based approaches (Gojcic *et al.*, 2021), the ICP matching does not search for corresponding object points in the existing sets of points, but creates new ones. Thus, the matching resolution is not restricted by the scanning resolution.

Moreover, based on the redundant observation of the virtual points within one epoch a realistic accuracy is estimated within the free network adjustment. Thus, also the significance tests within the subsequent deformation analysis give trustful results.

In comparison to the M3C2 algorithm, our approach also allows the detection of in-plane displacements. One requirement for that, however, is the use of suitable patches. The geometry of the structures has a major impact on the matching quality. It has to be unambiguous in the context of ICP matching. The geometry of a plane structure for example contains not enough information for a cloud-to-cloud match as the solution is ambiguous in the in-plane directions. This inevitably leads to incorrect point identities. It is therefore crucial to check the geometry of each selected structure beforehand. Besides others, two possible solutions could be:

a) Analysing the histogram of the normal vectors. If all normal vectors of a patch tend to point in the same direction or lay on a plane, the structure is not suitable for a reproducible matching. The more the normal directions vary the better the matching accuracy.
b) Estimating the matching accuracy of the ICP by simulating various displacements. This could be done within a Monte Carlo Simulation where the point cloud of the second epoch is shifted to different 3D starting positions and the accuracy of the matching outcome is analysed.

Apart from the structure's geometry, also other parameters like the scanning resolution affect the appearance of the point cloud and thus the matching accuracy (Wujanz, 2019). This includes, for example, also the measurement configuration between the structure and the two stations from which it is observed. If the viewing angle from the stations on the object is similar, the matching accuracy is potentially higher than when observing the structure from very different angles.

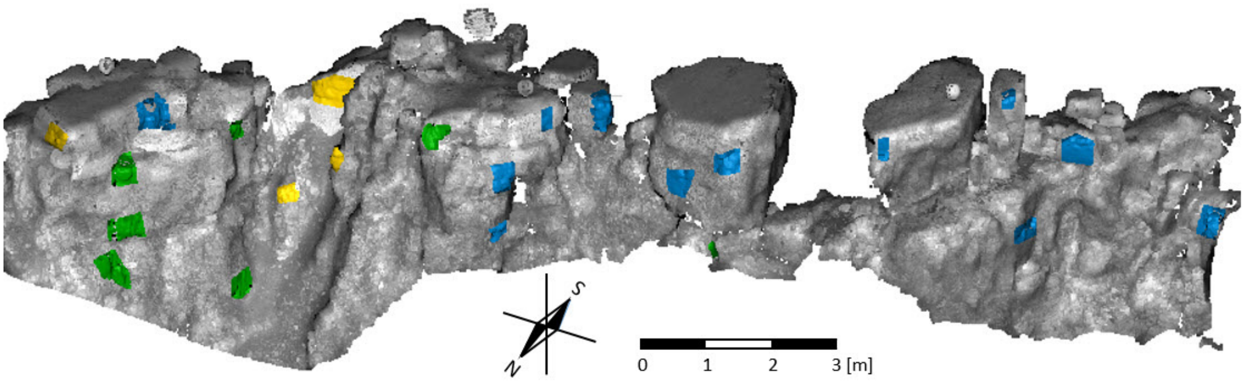

Figure 4. Point cloud of the southern, moving part of the cleft and manually selected patches (blue: station 1, yellow: station 2, green: both stations).

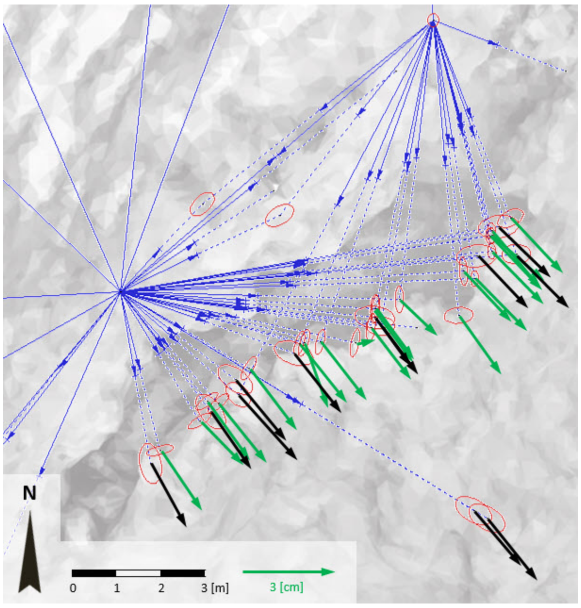

Figure 5. Resulting 2D deformation vectors of marked (black arrows) and virtual target points (green arrows) and their related error ellipses (red).

Those additional effects cannot be considered by analysing the normal histogram (solution a) of one point cloud. On the other hand, the Monte Carlo Simulation (option b) already takes the point cloud pair into account and directly analyses the outcome of the ICP matching. However, this will be investigated in future research.

Either way, the requirements on the structures limit the number of suitable patches. Nonetheless, on Mt. Hochvogel, a sufficient number of scan patches could be identified by a careful manual selection.

VI. Conclusion and Outlook

In this paper, we introduced and applied a new monitoring strategy extending the conventional network measurements by small-scale laser scans. This allows to increase the number of object points and thus the spatial resolution of the monitoring. By creating virtual target points based on ICP matching, we (i) solved the problem of missing point identities and (ii) estimated a suitable stochastic model by integrating them into the free network adjustment. As a result, we are able to perform a rigorous deformation analysis including a statistical significance test.

We applied our proposed method at the geo-monitoring of Mt. Hochvogel and were able to significantly increase the number of object points, especially in the inaccessible hazardous area. Moreover, the network geometry was improved and thus the accuracy of the network adjustment. Consequently, also the accuracy of the deformation vectors is higher and small deformations can be detected earlier. The deformation vectors resulting from virtual targets show the same movement as the vectors from marked network points.

However, there are some limitations. The number of useful structures and thus the spatial distribution of monitoring points, of course strongly depends on the object's surface. On very flat rock faces the identification of suitable patches might not be possible. Especially in these cases, an evaluation process that analyses the selected patches beforehand would help to ensure sufficient accuracy in the ICP matching. This will be investigated in future research also towards a fully automatic selection of patches in the point cloud.

VII. Acknowledgements

This research is done within the research project "AlpSenseRely" financed by the Bavarian State Ministry of the Environment and Consumer Protection.

References

Abellán, A., J.M. Vilaplana, J. Calvet, D. García-Sellés, and E. Asensio (2011). Rockfall monitoring by Terrestrial Laser Scanning – case study of the basaltic rock face at Castellfollit de la Roca (Catalonia, Spain). *Natural Hazards and Earth System Sciences*, Vol. 11, No. 3, pp. 829-841.

Akca, D. (2007). 3D Modelling, Texturing and Applications in Cultural Heritage. In: *Lecture notes for ISPRS WG VI/5 & summer school «Theory and Application of Laser Scanning»,* Ljubljana, Slovenia.

Anders, K., L. Winiwarter, H. Mara, R. Lindenbergh, S.E. Vos, and B. Höfle (2021). Fully automatic spatiotemporal segmentation of 3D LiDAR time series for the extraction of natural surface changes. *ISPRS Journal of Photogrammetry and Remote Sensing*, Vol. 173, No. 3, pp. 297-308.

Besl, P.J., and N.D. McKay (1992). Method for registration of 3-D shapes. *Sensor Fusion IV: Control Paradigms and Data Structures. International Society for Optics and Photonics,* Vol. 1611, pp. 586-607.

Frangez, V., E. Serantoni, and A. Wieser (2020). Geodetic Monitoring of Digitally Fabricated Structures Early After Construction. In: *Proc. of the FIG Working Week 2020,* Amsterdam, May 10-14, 10556.

Ge, X. (2016). *Terrestrial Laser Scanning Technology from Calibration to Registration with Respect to Deformation Monitoring.* Dissertation. Technical University of Munich.

Gojcic, Z., L. Schmid, and A. Wieser (2021). Dense 3D displacement vector fields for point cloud-based landslide monitoring. *Landslides*, Vol. 18, No. 12, pp. 3821-3832.

Gojcic, Z., C. Zhou, and A. Wieser (2019). Robust Pointwise Correspondences for Point Cloud based Deformation Monitoring of Natural Scenes. In: *Proc. of the 4th Joint International Symposium,* Athens, Greece, 15-17 May 2019.

Harmening, C., and H. Neuner (2016). Detecting Rigid Body Movements from TLS-based Areal Deformation Measurements. *Proc. of the 78th FIG Working Week 2016.*

Heunecke, O., H. Kuhlmann, W. Welsch, A. Eichhorn, and H. Neuner (2013). *Auswertung geodätischer Überwachungsmessungen*, 2nd ed. Berlin, Offenbach: Wichmann.

Holst, C., J. Janßen, B. Schmitz, M. Blome, M. Dercks, A. Schoch-Baumann, J. Blöthe, L. Schrott, H. Kuhlmann, and T. Medic (2021). Increasing Spatio-Temporal Resolution for Monitoring Alpine Solifluction Using Terrestrial Laser

Scanners and 3D Vector Fields. *Remote Sensing*, Vol. 13, No. 6, 1192.

Holst, C., and H. Kuhlmann (2016). Challenges and Present Fields of Action at Laser Scanner Based Deformation Analyses. *Journal of Applied Geodesy*, Vol. 10, No. 1, pp. 17-25.

Holst, C., B. Schmitz, and H. Kuhlmann (2017). Investigating the applicability of standard software packages for laser scanner based deformation analyses. In: *Proc. of the FIG Working Week,* Helsinki, Finland, 29 May–2 June.

Holst, C., P. Zeimetz, A. Nothnagel, W. Schauerte, and H. Kuhlmann (2012). Estimation of Focal Length Variations of a 100-m Radio Telescope's Main Reflector by Laser Scanner Measurements. *Journal of Surveying Engineering*, Vol. 138, No. 3, pp. 126-135.

Kenner, R., V. Gischig, Z. Gojcic, Y. Quéau, C. Kienholz, D. Figi, R. Thöny, and Y. Bonanomi (2022). The potential of point clouds for the analysis of rock kinematics in large slope instabilities: examples from the Swiss Alps: Brinzauls, Pizzo Cengalo and Spitze Stei. *Landslides*, Vol. 39, No. 4, p. 80.

Kromer, R.A., A. Abellán, D.J. Hutchinson, M. Lato, M.-A. Chanut, L. Dubois, and M. Jaboyedoff (2017). Automated terrestrial laser scanning with near-real-time change detection – monitoring of the Séchilienne landslide. *Earth Surface Dynamics*, Vol. 5, No. 2, pp. 293-310.

Kuhlmann, H., V. Schwieger, A. Wieser, and W. Niemeier (2014). Engineering Geodesy - Definition and Core Competencies. *Journal of Applied Geodesy*, Vol. 8, No. 4, pp. 327-334.

Lague, D., N. Brodu, and J. Leroux (2013). Accurate 3D comparison of complex topography with terrestrial laser scanner: Application to the Rangitikei canyon (N-Z). *ISPRS Journal of Photogrammetry and Remote Sensing*, Vol. 82, No. 2, pp. 10-26.

Leinauer, J., B. Jacobs, and M. Krautblatter (2020). Anticipating an imminent large rock slope failure at the Hochvogel (Allgäu Alps). *Geomechanics and Tunnelling*, Vol. 13, No. 6, pp. 597-603.

Lindenbergh, R., and P. Pietrzyk (2015). Change detection and deformation analysis using static and mobile laser scanning. *Applied Geomatics*, Vol. 7, No. 2, pp. 65-74.

Medić, T., H. Kuhlmann, and C. Holst (2020). Designing and Evaluating a User-Oriented Calibration Field for the Target-Based Self-Calibration of Panoramic Terrestrial Laser Scanners. *Remote Sensing*, Vol. 12, No. 1, 15.

Mukupa, W., G.W. Roberts, C.M. Hancock, and K. Al-Manasir (2016). A review of the use of terrestrial laser scanning application for change detection and deformation monitoring of structures. *Survey Review*, Vol. 36, No. 5, pp. 1-18.

Neuner, H., C. Holst, and H. Kuhlmann (2016). Overview on Current Modelling Strategies of Point Clouds for Deformation Analysis. *allgemeine vermessungs-nachrichten (avn)*, Vol. 123, 11-12, pp. 328-339.

Niemeier, W. (2008). *Ausgleichungsrechnung*: *Statistische Auswertemethoden*, 2nd ed. Berlin: de Gruyter.

Pelzer, H. (1971). Zur Analyse geodätischer Deformationsmessungen. *Deutsche Geodätische Kommission bei der Bayerischen Akademie der Wissenschaften Reihe C: Dissertationen, No.* 164.

Pfeiffer, J., T. Zieher, M. Bremer, V. Wichmann, and M. Rutzinger (2018). Derivation of Three-Dimensional Displacement Vectors from Multi-Temporal Long-Range Terrestrial Laser Scanning at the Reissenschuh Landslide (Tyrol, Austria). *Remote Sensing*, Vol. 10, No. 11, p. 1688.

Raffl, L., W. Wiedemann, and T. Wunderlich (2019). Non-signalized Structural Monitoring using Scanning Total Stations. In: *Proc. of the 4th Joint International Symposium,* Athens, Greece, 15-17 May.

Raffl, L., and T. Wunderlich (2020). Challenges and Hybrid Approaches in Alpine Rockslide Prevention - An alarming Case Study. In: *Proc. of the 8th INGEO International Conference on Engeneering Serveying & 4th SIG Symposium on Engeneering Geodesy,* Dubrovnik, Croatia.

Scaioni, M., L. Longoni, V. Melillo, and M. Papini (2014). Remote Sensing for Landslide Investigations: An Overview of Recent Achievements and Perspectives. *Remote Sensing*, Vol. 6, No. 10, pp. 9600-9652.

Schäfer, T., T. Weber, P. Kyrinovic, and M. Zamecnikova (2004). Deformation Measurement Using Terrestrial Laser Scanning at the Hydropower Station of Gabcikovo. In: *Proc. of INGEO 2004 and FIG Regional Central and Eastern European Conference on Engineering Surveying,* Bratislava, Slovakia.

Wagner, A. (2016). A new Approach for Geo-Monitoring using Modern Total Stations and RGB+D Images. *Measurement*, Vol. 82, pp. 64-74.

Welsch, W.M., and O. Heunecke (2001). Models and Terminology for the Analysis of Geodetic Monitoring Observations: Official Report of the Ad Hoc Committee WG 6.1. In: *Proc. of the 10th FIG International Symosium on Deformation Monitoring,* Orange, pp. 390-412.

Winiwarter, L., K. Anders, and B. Höfle (2021). M3C2-EP: Pushing the limits of 3D topographic point cloud change detection by error propagation. *ISPRS Journal of Photogrammetry and Remote Sensing*, Vol. 178, pp. 240-258.

Wujanz, D. (2016). *Terrestrial Laser Scanning for Geodetic Deformation Monitoring.* Dissertation. Technische Universität Berlin, Fakultät VI – Institut für Geodäsie und Geoinformationstechnik.

Wujanz, D. (2019). Araneo: Bestimmung eines erweiterten Unsicherheitsbudgets für die Deformationsmessung basierend auf terrestrischen Laserscans. *allgemeine vermessungs-nachrichten (avn)*, Vol. 126, No. 3, pp. 53-63.

Wujanz, D., M. Burger, M. Mettenleiter, and F. Neitzel (2017). An Intensity-based Stochastic Model for Terrestrial Laser Scanners. *ISPRS Journal of Photogrammetry and Remote Sensing*, Vol. 125, pp. 146-155.

Wunderlich, T., L. Raffl, and W. Wiedemann (2020). Creating Identities – Two Solutions for Rigorous Deformation Analysis of Areal Observations in Engineering Geodesy. *allgemeine vermessungs-nachrichten (avn)*, Vol. 127, No. 2, pp. 61-68.